JACS
JOURNAL OF THE AMERICAN CHEMICAL SOCIETY

Article

pubs.acs.org/JACS

It Takes More Than an Imine: The Role of the Central Atom on the Electron-Accepting Ability of Benzotriazole and Benzothiadiazole Oligomers

Dinesh G. (Dan) Patel, Fude Feng, Yu-ya Ohnishi,[†] Khalil A. Abboud, So Hirata,[†] Kirk S. Schanze,* and John R. Reynolds*[,#]

Department of Chemistry, Center for Macromolecular Science and Engineering, University of Florida, Gainesville, Florida 32611, United States

Supporting Information

ABSTRACT: We report on the comparison of the electronic and photophysical properties of a series of related donor−acceptor−donor oligomers incorporating the previously known 2*H*-benzo[*d*]-[1,2,3]triazole (**BTz**) moiety as the acceptor and the recently reported **BTzTD** acceptor, a hybrid of **BTz** and 2,1,3-benzothiadiazole (**BTD**). Although often implied in the polymer literature that **BTz** has good acceptor character, we show that this moiety is best described as a weak acceptor. We present electrochemical, computational, and photophysical evidence supporting our assertion that **BTzTD** is a strong electron acceptor while maintaining the alkylation ability of the **BTz** moiety. Our results show that the identity of the central atom (N or S) in the benzo-fused heterocyclic ring plays an important role in both the electron-accepting and the electron-donating ability of acceptor moieties with sulfur imparting a greater electron-accepting ability and nitrogen affording greater electron-donating character. We report on the X-ray crystal structure of a **BTzTD** trimer, which exhibits greater local aromatic character in the region of the triazole ring and contains an electron-deficient sulfur that imparts strong electron-accepting ability. Additionally, we examine the transient absorption spectra of **BTzTD** and **BTz** oligomers and report that the **BTz** core promotes efficient intersystem crossing to the triplet state, while the presence of the thiadiazole moiety in **BTzTD** leads to a negligible triplet yield. Additionally, while **BTz** does not function as a good acceptor, oligomers containing this moiety do function as excellent sensitizers for the generation of singlet oxygen.

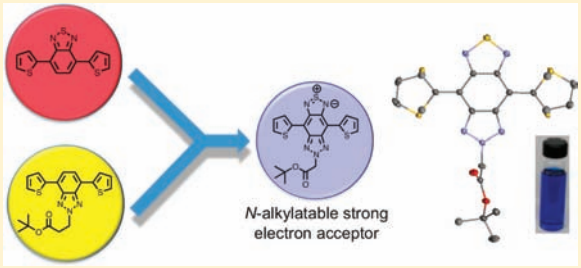

INTRODUCTION

Visible light absorbing conjugated polymers, oligomers, and small molecules are critical components for the efficient function of photonic devices. For example, solar energy conversion devices utilizing dye-sensitized nanostructured metal oxide thin films (dye-sensitized solar cells, DSSCs) have exceeded 10% efficiency,[1] while organic polymeric devices are fast approaching a similar metric.[2] In all-organic polymer and oligomer systems, visible light absorption can be achieved by the interaction of covalently linked, π-conjugated electron donor and electron acceptor groups,[3] and the wide variety of donor and acceptor units available allows for the tuning of electronic and optical properties.[4] This donor−acceptor (D−A) interaction, where the HOMO of the donor and the LUMO of the acceptor are largely responsible for the location of the frontier orbitals in the D−A system, is illustrated in Figure 1. The frontier orbitals in turn determine the light absorbing characteristics of the material.

In polymeric and oligomeric systems, 2,1,3-benzothiadiazole (**BTD**, Figure 1) and similar diimine containing units such as benzobis(thiadiazole) (**BBT**, Figure 1) are often employed as the acceptor because they can be coupled with donor units leading to easily polymerizable monomers. It is usually assumed that the polarizable imine unit is responsible for the electron-accepting character. The incorporation of long alkyl chains on the donor groups, however, is crucial to gain the required solubility necessary for solution processing, as these acceptors themselves cannot be symmetrically alkylated. Within the context of small molecule DSSCs, a large fraction of all-organic sensitizers rely on the cyanoacrylic acid group[5] (**CAA**, Figure 1), which acts as both the electron acceptor and the anchoring group to the metal oxide film. Because the **CAA** anchor is not a particularly strong acceptor,[6] such dyes typically incorporate additional acceptor moieties or have extended conjugation to shift the dye absorption maximum into the red region of the spectrum. Some research groups are now turning to stronger acceptors such as quinoxaline[7] and **BTD** to induce this spectral shift.[8] The use of **BTD**, however, necessitated a thiophene spacer containing the requisite carboxylate group for binding to titanium dioxide.[8]

Received: August 29, 2011
Published: January 31, 2012

   dx.doi.org/10.1021/ja207978v | *J. Am. Chem.Soc.* 2012, 134, 2599−2612

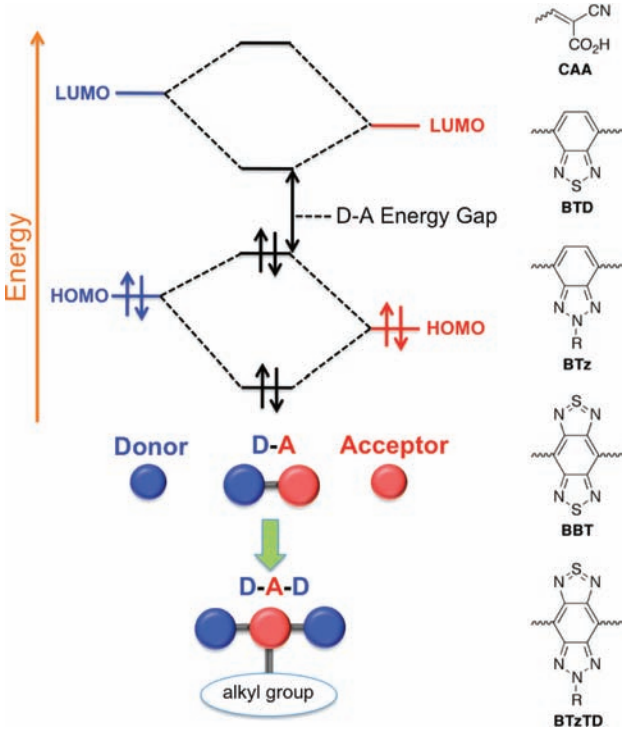

Figure 1. Energy level diagram showing how the molecular oribtals of a donor and acceptor interact in a D−A system with a reduced HOMO−LUMO gap. Also shown are the molecular structures of the cyanoacrylic acid (**CA**) acceptor and anchoring group commonly used in DSSCs, the benzothiadiazole (**BTD**) acceptor, the benzotriazole (**BTz**) moiety, the benzobis(thiadiazole) (**BBT**) acceptor, and the benzo(triazole-thiadiazole) (**BTzTD**) hybrid acceptor.

We were interested in the use of symmetric, alkylatable electron acceptors as part of our larger research program on visible light absorbing conjugated poly- and oligo-electrolytes. Our investigation began using the benzotriazole moiety (**BTz**, Figure 1) because of the potential for alkylation at the central nitrogen and because recent reports suggest that in polymer systems it is electron deficient and therefore acts as an electron-accepting moiety.[9] As part of this present study, however, we report that **BTz** does not function as a particularly strong electron acceptor, which resulted in our design and synthesis, simultaneously with the Grimsdale group,[10] of a new acceptor, benzo(triazole-thiadiazole), which is a hybrid of **BTD** and **BTz** and that we abbreviate as **BTzTD**.

The study herein combines experimental and comprehensive computational data, which we show calls into question the conventional idea that inclusion of an imine or diimine group in the molecular framework of a π-conjugated system will necessarily lead to strong electron-accepting ability. We show that the identity of the central atom in benzofused systems, such as those presented here, is of critical importance in determining the LUMO energy level but also has a surprising effect on the HOMO level in D−A systems as well. While Grimsdale[10] and others[11] have discussed the HOMO level for sulfur, selenium, and tellurium containing **BTD** and **BBT** analogues, a crucial qualitative and quantitative discussion comparing sulfur and nitrogen analogues (**BTz** vs **BTD** and **BTzTD** vs **BBT**) has not yet been put forth, and this is important given that they are more stable and more commonly found in organic materials than their selenium and tellurium analogues.

The new **BTzTD** acceptor introduced by Grimsdale's group[10] and ours helps fill a gap in that it is a strong electron acceptor and is capable of further functionalization via *N*-alkylation; therefore, we believe it will find much utility in organic electronics. Importantly, our route introduces the nitration of **BTD** before any acid labile groups are introduced, while the Grimsdale route subjects the substituted **BTz** moiety to nitration; therefore, acid-sensitive groups (such as those used for binding to metal oxides) cannot be used as substituents using the latter approach. As an example, esters, silanes, and alcohols are relevant if **BTzTD** containing oligomers and polymers are to find use in surface modification applications and as other materials such as conjugated polyelectrolytes. In our study, the photophysical and electrochemical properties of ester-substituted **BTzTD** are put into perspective by comparison of its properties to analogous oligomers containing **BTz**, **BTD**, **BBT**, and tetrazine (oligomer **7**) cores. We abbreviate the tetrazine core as **TZ** and use it for comparison purposes in our study. The family of oligomers under study is collectively shown in Chart 1.

Chart 1. Molecular Structures of BTz (Series 1 Compounds and Compound 3), BTzTD (Series 2 Compounds and Compound 4), BTD (5), BBT (6), and Tetrazine (7)-Containing Oligomers[a]

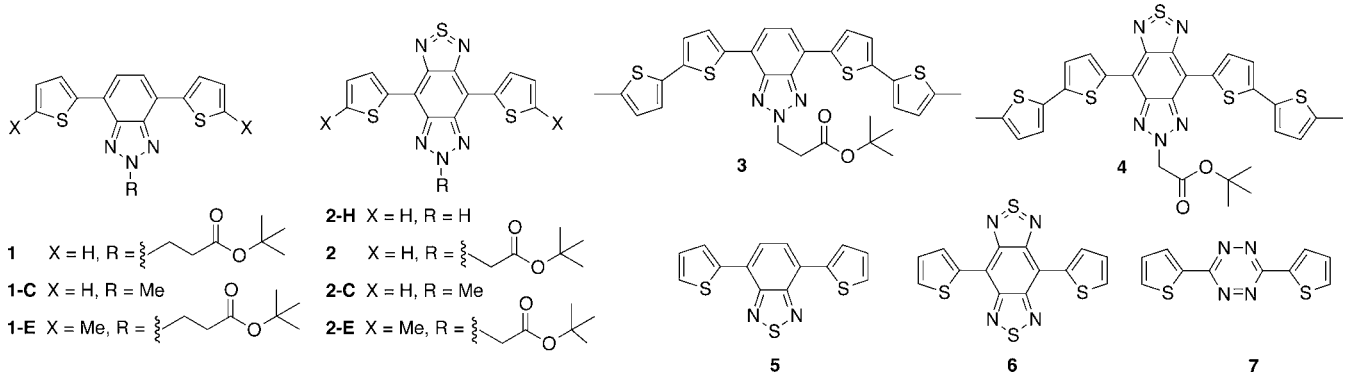

[a]The hyphenated **C**, **E**, and **H** descriptors are used to denote oligomers used for computations, electrochemistry experiments, and those that are unalkylated, respectively.

dx.doi.org/10.1021/ja207978v | *J. Am. Chem.Soc.* 2012, 134, 2599−2612

RESULTS AND DISCUSSION

Synthetic Design. The **BTz** moiety has been explored as an acceptor only within the past few years, usually within the context of polymeric systems.[9] The groups of Toppare[9a−c,12] and others[9e] have reported direct bromination of *N*-alkylated **BTz** to allow for subsequent metal-catalyzed coupling reactions in the construction of monomer units.[9b] We found that an indirect procedure utilizing commercially available 2,1,3-benzothiadiazole (**8**) as a precursor for **BTz** oligomers gave high product yield and purity in our hands. As outlined in Scheme 1, **8** is brominated giving 4,7-dibromobenzo[*c*][1,2,5]-thiadiazole (**9**), which is reduced with sodium borohydride in ethanol to give 1,2-diamino-3,6-dibromobenzene (**10**).[13] Compound **10** is then cyclized under acidic conditions with sodium nitrite to give the asymmetric dibrominated benzotriazole **11**.[9f] We assign this asymmetric structure based on the ^{1}H and ^{13}C NMR spectra of this compound. To alkylate **11**, we chose to use the aza-Michael addition reaction employing *tert*-butyl protected acrylic acid and *N*,*N*-dimethylaminopyridine catalyst, for which there is literature precedence.[14] This reaction is reversible and, as a consequence of **BTz** functioning as a good leaving group,[15] only afforded the alkylated product in moderate yield. We were able to isolate desired symmetric product **12a** in 53% yield, while the asymmetric product **12b** was obtained in 6% yield. We surmise that the bromine atoms in **11** sterically hinder the benzylic nitrogen atoms, thus inhibiting reaction at those sites and affording **12a** as the major product. Compound **12a** can be coupled with commercially available 2-(tributylstannyl)thiophene under Stille conditions to give trimer **1**. Because **12b** forms in lower yield, we chose not to pursue oligomers based on this asymmetric **BTz** core. Trimer **1** is brominated with *N*-bromosuccinimide (NBS) in chloroform to give dibrominated compound **13**, which is then coupled with 2-methyl-5-(trimethylstannyl)thiophene[16] under Stille conditions to give pentamer **3**.

Scheme 1. Synthetic Route to BTz Oligomers 1 and 3

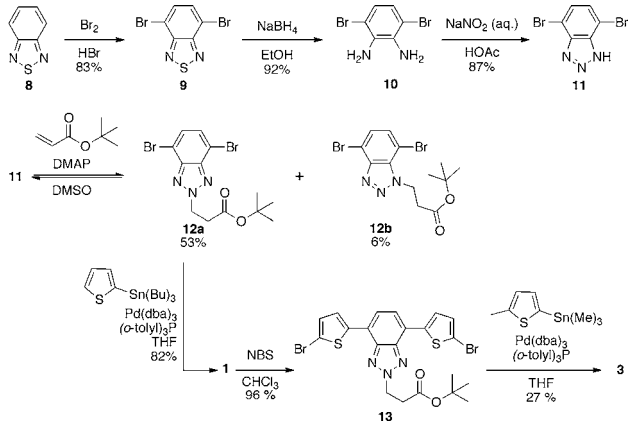

The aforementioned oligomers were appealing because they have the ability both for symmetric *N*-alkylation on the acceptor and for symmetric disubstitution with aromatic donor moieties in keeping with our desire for conjugated D−A−D type systems. Equally important for our design goals is the ability of these D−A−D systems to efficiently absorb long wavelength visible light. Preliminary spectral and electrochemical experiments suggested that oligomers incorporating the **BTz** acceptor would not fulfill the second half of our design goals. Accordingly, we noted that synthetically the **BTz**, **BTD**, and **BBT** moieties are accessible via *ortho*-diaminobenzene (*o*-DAB) precursors (compound **10** for **BTz** and **BTD** and compound **16** for **BBT** in Schemes 1 and 2). To arrive at **BTD** or **BBT**, the appropriate precursor is treated with thionyl chloride[13] or *N*-thionylaniline in pyridine.[17] If compound **16** were instead treated with sodium nitrite under acidic conditions, a **BTzTD** containing oligomer would be obtained. Given that **BTzTD** contains the strongly accepting **BTD** moiety, effectively a hybrid of **BTD** and **BTz**, we hoped that it would fulfill our design goals.

Scheme 2. Synthetic Route to Alkylated BTzTD Containing Trimers 2-H and 2

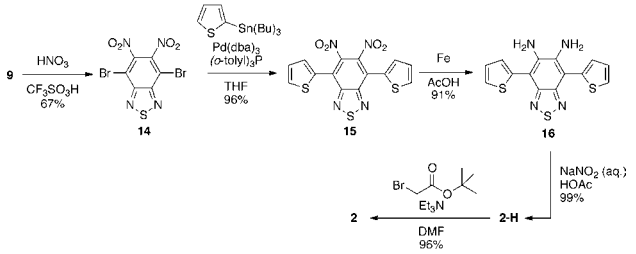

The synthesis of **BTzTD** containing oligomers **2-H** and **2** is outlined in Scheme 2. We use the descriptor **H** to indicate that the acceptor is in its protonated, unalkylated form. As with **BTz**, dibrominated compound **9** is a key precursor. Compound **9** is nitrated to give **14** using a mixture of fuming nitric acid and fuming sulfuric acid[17,18] or via a new nitration route developed by Andersson and co-workers,[19] which employs fuming nitric and trifluoromethane sulfonic acids. This new route affords higher yields and obviates the need for tedious chromatography to separate **14** from the mononitrated side product. We next use Stille methodology to couple **14** with 2-(tributylstannyl)-thiophene to afford trimer **15**.[17] The nitro groups are reduced using iron powder in acetic acid to give diamino-trimer **16**,[17,20] which, as mentioned earlier, is similar to the precursor required for **BBT** compounds. Trimer **16** is cyclized using sodium nitrite in acetic acid[9f] to give the unalkylated **BTzTD** trimer **2-H**. Compound **2-H** is a maroon colored solid with limited solubility in common organic solvents. Fortuitously, and unlike molecule **11**, trimer **2-H** has C_{2h} symmetry that allows for alkylation yielding a single symmetric product. We assign this symmetric structure for **2-H** based on ^{1}H and ^{13}C NMR spectra.

To alkylate the **BTzTD** acceptor core, we initially tried using the aza-Michael addition that had succeded in giving **BTz** containing oligomers **12a** and **12b**. We found that the reaction proceeded sluggishly, and attempts to drive the reaction toward the product by adding excess *t*-butyl acrylate gave complicated NMR spectra. Analysis of the crude material by mass spectrometry suggests that adding excess acrylate leads to the formation of **BTzTD** initiated acrylate oligomers. This oligomeric mixture was not characterized further. The reversibility of the aza-Michael addition coupled with the enhanced electron-accepting ability, and therefore stability of deprotonated **2-H**, likely meant that the equilibrium tended toward the starting material. To circumvent this, we hoped that a deprotonation step followed by an S_N2 reaction with a halogenated *t*-butyl protected carboxylic acid would afford the desired alkylated oligomer. In fact, this route worked in near

dx.doi.org/10.1021/ja207978v | J. Am. Chem.Soc. 2012, 134, 2599−2612

quantitative yield when employing triethylamine as the base in DMF solvent to give alkylated oligomer **2** (Scheme 2). The alkylated oligomer **2** is dark blue in color.

Synthesis of oligomer **4** (Scheme 3) proceeds by bromination of **15** with NBS using an acetonitrile/DMF

Scheme 3. Synthesis of BTzTD Containing Oligomer 4

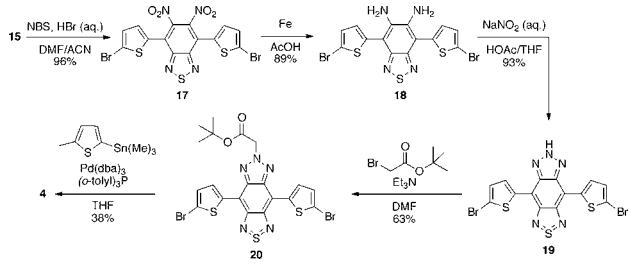

solvent system.[20] Catalytic aqueous HBr helps drive the reaction. Reduction of the resulting dibromo compound **17**[20] is effected in acetic acid using iron powder, and resulting diamine **18** is cyclized using sodium nitrite in acetic acid to give oligomer **19**. The alkylation of **19** in DMF and promoted by triethylamine gives **20**, which is coupled under Stille conditions with 5-methyl-2-trimethylstanylthiophene to give oligomer **4**. Oligomer **4** is slightly soluble in chlorinated solvents and THF. Purification is achieved first by column chromatography, and then reprecipitation of a concentrated chloroform solution of **4** into rapidly stirring hot hexane.

For electrochemical characterization, methyl terminated pentamers **3** and **4** are used in addition to methyl terminated trimers **1-E** and **2-E** (shown in Chart 1). The synthesis of **1-E** and **2-E** is detailed in the Supporting Information. Methylation at the terminal α-position on the thiophene rings prevents polymerization during the cyclic voltammetry (CV) and differential pulse voltammetry (DPV) experiments used to assign the HOMO and LUMO energies.[21]

Computational Analysis: Part 1. In tandem with our synthetic efforts, we computationally analyzed and compared a series of five oligomers that include the well-known **BTD** (oligomer **5**) and **BBT** (oligomer **6**) acceptors as well as methylated **BTz** and **BTzTD** containing oligomers **1-C** and **2-C** (Chart 1). We chose density functional theory (DFT) methods, known to have a good balance between accuracy and the computational time required.[22] Methyl substituents were chosen to simplify the computations with the computational details supplied in the Experimental Section. Tetrazine (**TZ**) containing oligomer **7**[23] (Chart 1) was examined for comparison purposes because it contains only electron-withdrawing imine nitrogens and does not include trivalent nitrogen or divalent sulfur atoms as part of a fused heterocyclic ring. As we shall show, the presence and identity of the central atom (N or S in **BTz** or **BTD**) has a substantial impact on the LUMO level, and, surprisingly, also the HOMO level of the oligomeric system.

The HOMO and LUMO levels obtained computationally in the gas phase are summarized in Figure 2. It is noted that while both the HOMO and the LUMO values computed in dichloromethane using the polarized continuum model (PCM) are slightly lower than those in vacuo, the trends of these values in dichloromethane parallel those in vacuo. These exact numerical values are given in the Supporting Information.

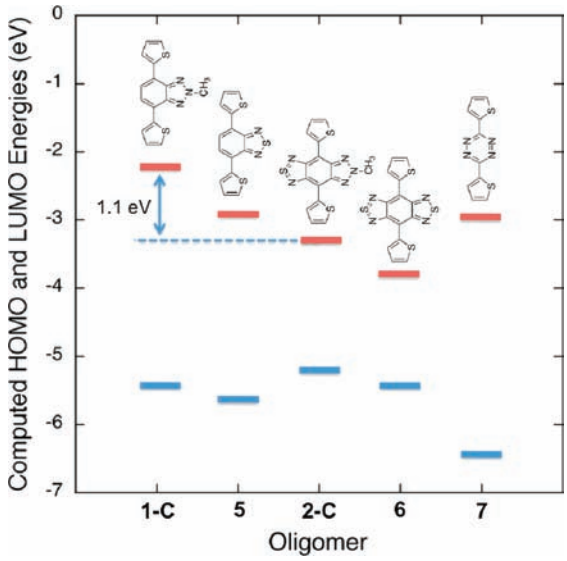

Figure 2. Graphical representation of the gas-phase calculated HOMO and LUMO values for oligomers **1-C**, **2-C**, and **5**−**7**.

For the discussions that follow, we will mainly discuss the values in vacuo.

Using the calculated LUMO level as a crude predictor of electron-accepting ability[24] in accordance with Koopmans' theorem, the computational trends show that **BTz** oligomer **1-C** is a weak electron acceptor. Its calculated LUMO level, at −2.23 eV, is higher than **BTD** containing oligomer **5**, the next weakest acceptor, by 0.66 eV. While oligomers **1-C** and **5** are isoelectronic, it is clear from both our experimental results and the computations that the substitution of NCH_3 for S has a profound impact on the electron-accepting ability with sulfur imparting greater electron-accepting character as we detail below. Notably, the results for **BTzTD** oligomer **2-C** are encouraging as the LUMO level calculated for this oligomer is between that of the **BTD** and **BBT** oligomers and considerably lower than that for the **BTz** oligomer. Consequently, we believe that **BTzTD** would indeed make a good electron acceptor. On the basis of our computations, we assign acceptor strength as **BTz** < **BTD** < **TZ** < **BTzTD** < **BBT**.

Oligomers: Spectral Characterization. In a polymeric context, **BTz** has been used as an electron acceptor to afford polymers that absorb in the visible region of the electromagnetic spectrum.[9,25] Initially, we reasoned that **BTz** would also function as an acceptor in oligomeric systems given that it has an electron-accepting diimine component as part of its benzannulated structure. A recent report by You and coworkers,[25] however, points out that the electron-rich nature of **BTz** results in an increase in the LUMO level, thus decreasing its electron-accepting ability. No references were provided for this premise, however. Our own expeiments presented here, including spectral data and electrochemical measurements, suggest that **BTz** acts more as an electron neutral, rather than electron accepting, moiety in oligomeric systems. In polymeric systems, we believe that **BTz** presents the appearance of a good electron acceptor because of the band structure and decrease of the HOMO−LUMO gap that results when oligomeric units are brought together to give extended conjugated structures.

In methylene chloride solution, **BTz** oligomer **1** has an absorption band in the near-UV region with λ_{max} at 278 and 387 nm and an absorption band edge at 440 nm (Figure 3,

dx.doi.org/10.1021/ja207978v | J. Am. Chem.Soc. 2012, 134, 2599−2612

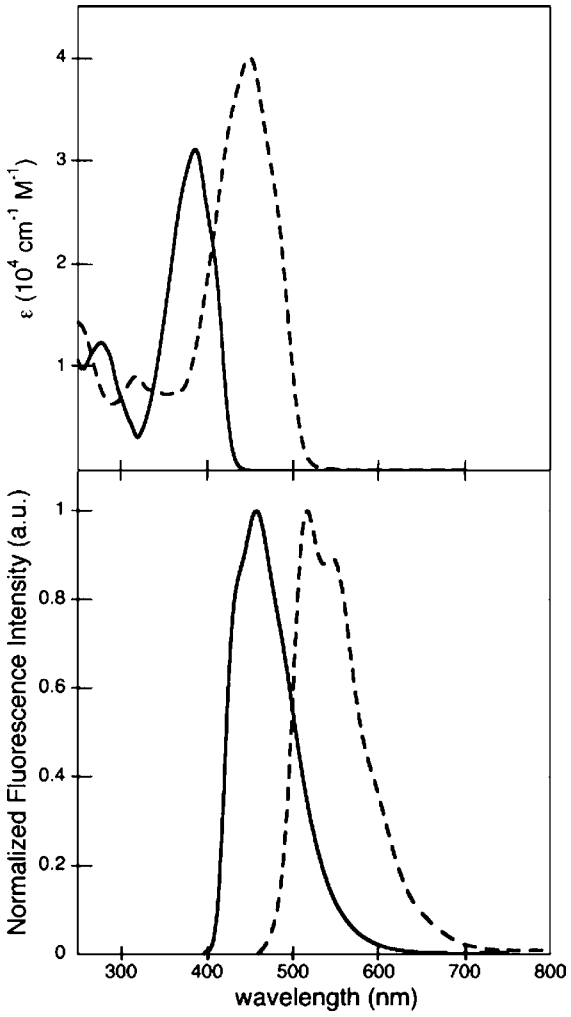

Figure 3. Absorption (top) and normalized emission (bottom) spectra of oligomers **1** (—) and **3** (– – –) in methylene chloride solution.

top). We ascribe the 287 nm band to a transition polarized along the short axis of the molecule, while the 387 nm absorption band is due to a long-axis transition analogous to what was proposed by Fraind and Tovar[26] for a thiophene–anthracene–thiophene trimer. For comparison, terthiophene has a long wavelength absorption maximum at 355 nm in chloroform solution, with a shorter wavelength transition at 245 nm.[27] Oligomer **1**, in methylene chloride solution, is also fluorescent with λ_{em} at 456 nm and a quantum yield of 0.44 in ethanol when using coumarin 480 as the actinometer[28] (Figure 3). These high-energy transitions suggest that the donor–acceptor interaction is minimal in this three-ring oligomer.

For use in organic photonic devices, a material must be able to adequately absorb in the longer wavelength region of the visible spectrum. As oligomer **1** does not effectively accomplish this goal, we sought to decrease the energy of the absorption band of **BTz** containing oligomers by extending the conjugation through successive addition of donor groups. Oligomer **3** is a pentamer where the **BTz** core is flanked by a total of four thiophene donor units. The absorption of **3** in methylene chloride shows two major bands with λ_{max} values of 320 and 450 nm (Figure 3). The absorption band edge appears at approximately 512 nm. Additionally, oligomer **3** shows fluorescence emission with emission maxima at 516 and 546 nm with a quantum yield of 0.32 when using coumarin 480 as the actinometer.[28] While the observed changes in the absorption spectra on going from **1** and **3** are consistent with a molecular structure containing extended conjugation, a significant portion of the absorptive transitions still occurs in the UV region.

Given the position of the absorption maxima, the absorption spectra for both **1** and **3** do not appear to be consistent with a D–A–D type structure where there is effective charge transfer, leading us to conclude that shorter **BTz** containing oligomers will likely not make effective visible light absorbing chromophores, despite the peak extinction coefficients of 3.1×10^4 and 4.0×10^4 M^{-1} cm^{-1}, for **1** and **3**, respectively.

By contrast to the properties of **BTz**-based oligomers, the **BTzTD**-based oligomers exhibit spectral features as predicted by the computations, with transitions in the long wavelength region of the visible and near-infrared (NIR) spectrum,

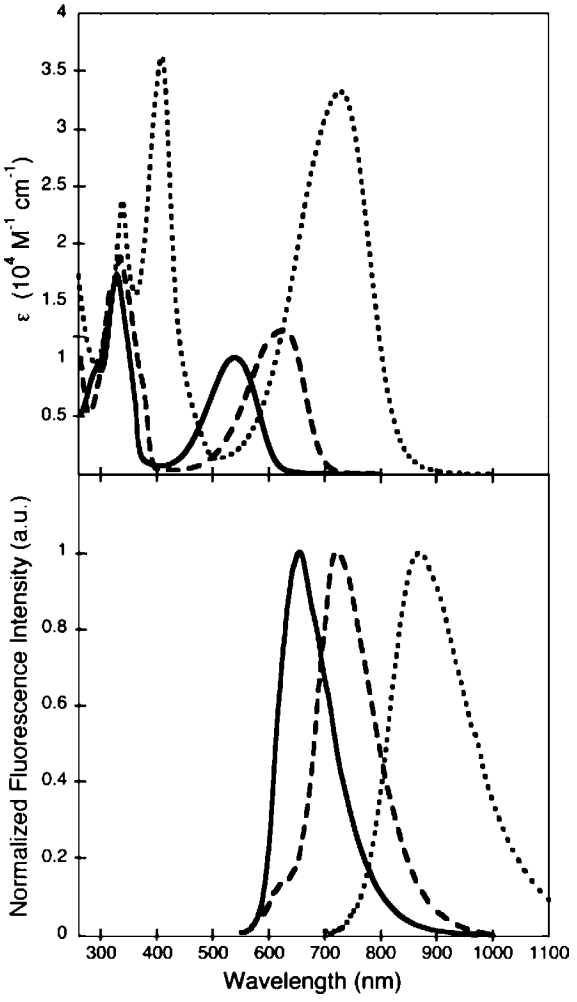

Figure 4. Absorption (top) and emission (bottom) spectra of oligomer **2-H** (—), **2** (– – –), and **4** (···) in methylene chloride.

indicating they have comparatively small HOMO–LUMO gaps. In particular, in methylene chloride solution, unalkylated oligomer **2-H** has absorption maxima at 330 and 540 nm (Figure 4, top). The prominent charge transfer band is well-defined and separated from the higher energy absorption band, which we attribute to a short-axis transition due to the **BTzTD** moiety. Similar to **BTz** oligomers **1** and **3**, we attribute the short wavelength absorption to a transition along the short axis

dx.doi.org/10.1021/ja207978v | J. Am. Chem.Soc. 2012, 134, 2599–2612

Table 1. Electrochemical Data for D−A−D Oligomers

oligomer	acceptor	$E_{1/2}^{ox}$ (V)	$E_{1/2}^{red}$ (V)	E_{ox}^{onset} (V)	E_{red}^{onset} (V)	HOMO (eV)	LUMO (eV)	ref
1-E	**BTz**[a,b]	0.55	−2.44	0.42	−2.30	−5.54	−2.82	*c*
				(0.38)	(−2.25)	(−5.50)	(−2.87)	
						[−5.44]	[−2.23]	
3	**BTz**[a,b]	0.32	−2.23	0.20	−2.13	−5.32	−2.99	*c*
				(0.12)	(−2.06)	(−5.24)	(−3.06)	
2-E	**BTzTD**[a]	0.38	−1.37	0.22	−1.27	−5.34	−3.85	*c*
				(0.13)	(−1.20)	(−5.25)	(−3.92)	
						[−5.23]	[−3.25]	
4	**BTzTD**[a]	0.20	−1.26	0.05	−1.23	−5.17	−3.89	*c*
				(−0.07)	(−1.15)	(−5.05)	(−3.97)	
5	**BTD**[d]	—[g]	−1.68	0.78	−1.63	−5.90	−3.49	30
						[−5.66]	[−2.89]	
6	**BBT**[e]	—[g]	−0.93	0.55	−0.84	−5.32	−4.28	31
						[−5.40]	[−3.78]	
7	**TZ**[f]	—[g]	−1.22	1.18	−1.02	−7.30	−4.10	23
						[−6.43]	[−2.95]	

[a]Energies are reported relative to the Fc/Fc^+ redox couple and are obtained from CV experiments with the corresponding DPV experiment values shown in parentheses and the energies computed by DFT methods in this work shown in brackets; the solvent employed is dichloromethane unless otherwise noted. [b]Values are obtained from THF solutions with the exception of the $E_{1/2}^{ox}$ values, which are obtained from dichloromethane solutions. [c]Values are from data presented in this work. [d]Values are obtained by CV in CH_2Cl_2 solution; an SCE reference electrode calibrated against Fc/Fc^+ was used; the onset of oxidation and reduction defines the HOMO and LUMO levels, respectively. [e]Values are obtained by CV in benzonitrile solution; an SCE reference electrode was used; the onset of oxidation and reduction defines the HOMO and LUMO levels, respectively. The value $E_{1/2}^{red}$ and onset values reported here are converted to vs Fc/Fc^+. [f]The LUMO value is obtained by CV in dichloromethane solution using an Ag/AgCl reference electrode; the HOMO is calculated using the onset of absorption added to the LUMO level. The onset values reported here have been converted to vs Fc/Fc^+. [g]Half-wave potentials were not provided as the oxidation was not reversible.

of the molecule.[26] Oligomer **2-H** fluoresces with λ_{em} at 659 nm and a quantum yield of 0.87 when using 3,3′-diethyloxadicarbocyanine iodide in ethanol as the actinometer (Figure 4, bottom).

Upon alkylation of oligomer **2-H** to give **2**, we observe a significant bathrochromic shift in the charge transfer band that has a peak at 630 nm, while the higher energy band is only shifted by 6 nm and is now at 336 nm (Figure 4, top). Oligomer **2** fluoresces with λ_{em} at 723 nm and a quantum yield of 0.57, also with 3,3′-diethyloxadicarbocyanine iodide in ethanol as the actinometer (Figure 4, bottom). As with **2-H**, the two absorption bands are well-defined with no overlap. The onset of absorption for **2** is 730 nm (1.7 eV), close to the DFT computed HOMO−LUMO gap of 2.03 eV in dichloromethane. When comparing the absorption spectra of **2-H** and **2** to **BTz** analogue **1**, it is clear that there is greater charge transfer character associated with the **BTzTD** containing systems.

Extension of the conjugation length and moving from oligomer **2** to oligomer **4** is accompanied by a further red-shift in the absorption maxiumum. Oligomer **4** shows three well-defined absorption transitions at 338, 409, and 729 nm and has a fluorescence maximum at 870 nm (Figure 4). A fluorescence quantum yield of 0.06 is measured when using ZnTPP as the actinometer.[29] Worthy of note is the fact that oligomer **4** exhibits low solubility in most polar organic solvents, but even when present at low concentration it produced darkly colored solutions due to its high extinction coefficient (3.6×10^4 M^{-1} cm^{-1} at 409 nm and 3.3×10^4 M^{-1} cm^{-1} at 729 nm).

Oligomers: Electrochemical Characterization. To characterize the oligomers under study, we utilize both cyclic voltammetry (CV) and differential pulse voltammetry (DPV) methods and assign the half-wave potentials versus the ferrocene−ferrocenium (Fc/Fc^+) redox couple as is common in the literature. Because the D−A−D oligomers in our work may also find utility in solid-state devices such as solar cells, we also present data on the onset of oxidation and reduction versus Fc/Fc^+ and on the absolute values of the HOMO and LUMO levels relative to vacuum. As such, the results presented may be used for direct comparisons with existing D−A molecules. A compilation of the electrochemical data is given in Table 1.

Our analysis began with oligomers **1-E** and **3** in dilute methylene chloride solution using a platinum button working electrode, nonaqueous $Ag/AgNO_3$ reference electrode, and a platinum flag counter electrode with tetrabutylammonium hexafluorophosphate as the supporting electrolyte. We observed that the solvent/electrolyte system reduced before any reductive processes associated with the oligomers. Specifically, sweeping the potential from 0 to −2.25 V vs Fc/Fc^+ gave rise to a sharp increase in current flow, but this was observed regardless of whether or not the oligomers were present in solution.

While not commonly used as a solvent for electrochemical experiments, THF does allow access to a larger electrochemical window for reductive processes.[32] With this in mind, both **1-E** and **3** were examined in THF solution and exhibit reductive processes by CV. Both compounds were also examined by DPV, and these data are presented in Figure 5. By CV, oligomer **1-E** shows quasi-reversible reduction centered at −2.44 V versus Fc/Fc^+ (onset of reduction at −2.30 V by CV and −2.26 V by DPV). Oligomer **3** also exhibits a quasi-reversible reduction centered at −2.23 V versus Fc/Fc^+ (onset of reduction at −2.13 V by CV and −2.06 V by DPV). In summary, the electrochemistry shows that that **BTz** oligomers **1-E** and **3** have relatively high energy LUMO levels as reflected by the especially negative cathodic reduction potentials.

The HOMO level of each **BTz** oligomer was also investigated electrochemically (Figure 5). In THF solution, oligomer **1-E** shows an irreversible oxidation wave with an onset at approximately 0.42 V by CV (0.38 V by DPV). In

dx.doi.org/10.1021/ja207978v | J. Am. Chem.Soc. 2012, 134, 2599−2612

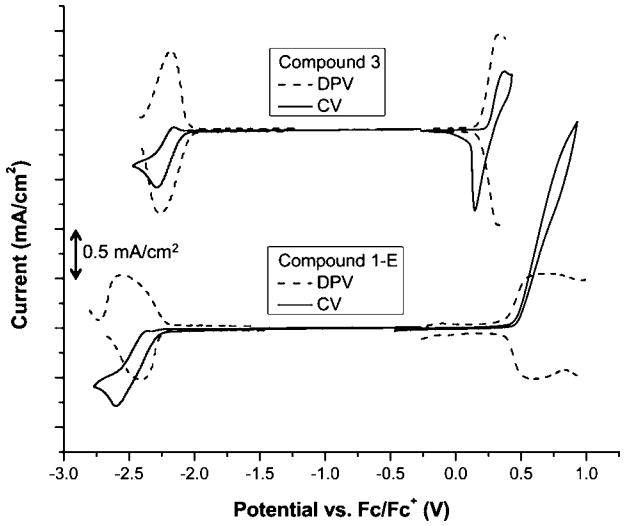

Figure 5. Cyclic voltammetry (CV, solid lines) and differential pulse voltammetry (DPV, dashed lines) data for for **1-E** (bottom) and **3** (top). The data were obtained in THF solution at 5 mM concentration using 0.1 M tetrabutylammonium hexafluorophosphate as the supporting electrolyte, a platinum button working electrode, a nonaqueous $Ag/AgNO_3$ reference electrode, and a platinum flag counter electrode. The scan rate was 20 mV/s.

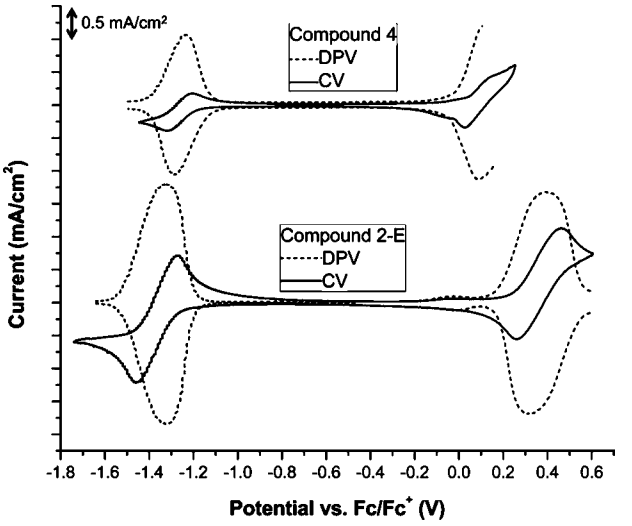

Figure 6. Cyclic voltammetry (CV, solid lines) and differential pulse voltammetry (DPV, dashed lines) data for for **2-E** (bottom) and **4** (top). The data were obtained in dichloromethane solution at 5 mM concentration using 0.1 M tetrabutylammonium hexafluorophosphate as the supporting electrolyte, a platinum button working electrode, a nonaqueous $Ag/AgNO_3$ reference electrode, and a platinum flag counter electrode. The scan rate was 20 mV/s for **2-E** and 50 mV/s for **4**.

contrast, oligomer **3** shows a quasi-reversible oxidation centered at 0.25 V (onset of oxidation at 0.20 V by CV and 0.12 V by DPV). The lower potential required to oxidize **3** when compared to **1-E** is consistent with a system that is more conjugated. Interestingly, **1-E** and **3** both show reversible oxidation in methylene chloride solution with their oxidation onsets being 0.48 and 0.28 V, respectively, by CV (Supporting Information, Figure S1), similar to the THF figures. The $E_{1/2}^{ox}$ value for **1-E** in methylene chloride is 0.55 V, while the value for **3** is 0.32 V. The fact that the oxidation process for **1-E** is fully reversible in methylene chloride but not in THF implies that THF reacts with the cation radical, possibly by acting as a nucleophile or as a base to promote decomposition.

The electrochemical results for oligomers **1-E** and **3** are summarized in Table 1 along with values for oligomers **2-E** and **4**, which will be discussed shortly. With both spectral and electrochemical evidence suggesting that **BTz** containing oligomers would not function as effective visible light absorbing materials, we turned our attention to **BTzTD** containing oligomers.

When examined by CV and DPV in methylene chloride, **BTzTD** oligomers **2-E** and **4** show reversible or quasi-reversible oxidative and reductive processes (Figure 6). Compound **2-E** has a reversible oxidation with $E_{1/2}^{ox}$ of 0.38 V vs Fc/Fc^+ (onset at 0.22 V by CV and 0.13 V by DPV). Upon extension of the donor portion, compound **4** shows quasi-reverisble oxidation at a lower potential centered at 0.20 V vs Fc/Fc^+ (onset at 0.05 V by CV and −0.07 V by DPV). Remarkably, both **2-E** and **4** exhibit lower oxidation potentials when compared to their **BTz** analogues, **1-E** and **3**. Compounds **2-E** and **4** both show reversible reduction with $E_{1/2}^{red}$ values of −1.37 and −1.26 V, respectively, vs Fc/Fc^+. The onset of reduction for **2-E** is −1.27 V by CV (1.20 V by DPV), while the onset for **4** is −1.23 V by CV (−1.15 V by DPV). In summary, the **BTzTD** oligomers both show lower reduction potentials than the **BTz** oligomers.

Electrochemically, both of the **BTzTD** oligomers under examination have reduced energy gaps when compared to their **BTz** analogues. The electrochemical energy gap, defined as the difference between the onset of oxidation and reduction, is thus determined to be 1.49 eV by CV and 1.33 eV by DPV for **2-E**. These values are smaller than the HOMO−LUMO gap determined by DFT (2.03 eV) and the optical energy gap determined experimentally (1.7 eV). The discrepancy with the computed values can be accounted for by solvation effects, which are expected to reduce the value of E_g by stabilizing the molecular dipoles in both the ground and the excited states. The HOMO−LUMO energy gap for oligomer **4** was not computed by DFT methods, although the electrochemical data gives a HOMO−LUMO gap of 1.28 eV with the corresponding optical energy gap being 1.4 eV.

The compilation of our experimental electrochemical results as well as the data previously reported for **5**, **6**, and **7** is also given in Table 1. The onset potentials are used to estimate the HOMO and LUMO values relative to vacuum level for the oligomers by using the conversion HOMO (eV) = E_{onset}^{ox} + 5.12 V and LUMO (eV) = E_{onset}^{red} + 5.12 V.[33] Worthy of note is the difference between the HOMO levels of **1-E** and **2-E**. The more electron-rich oligomer **1-E** would be predicted to be easier to oxidize relative to **2-E**, which incorporates the better electron-accepting **BTzTD** group. However, **2-E** is easier to oxidize by about 0.2 V. This supports the notion that **BTzTD** is not only a strong electron-accepting group, but also functions as an effective electron-donating group. The enhanced electron-donating ability of **BTzTD** relative to **BTz** was predicted by our DFT calculations. As stated earlier, and based on crystallographic and computational evidence (vide infra), the electron donation is likely enhanced due to the combined effects of the alkylated central nitrogen, which imparts "pyrrole-like" electron donor character to the hybrid acceptor, and the electropositive sulfur atom. The electron-accepting order predicted by DFT methods parallels the order obtained experimentally. Furthermore, computations correctly predicted that **7** would have the lowest energy HOMO, a fact confirmed by experiment.

dx.doi.org/10.1021/ja207978v | J. Am. Chem.Soc. 2012, 134, 2599−2612

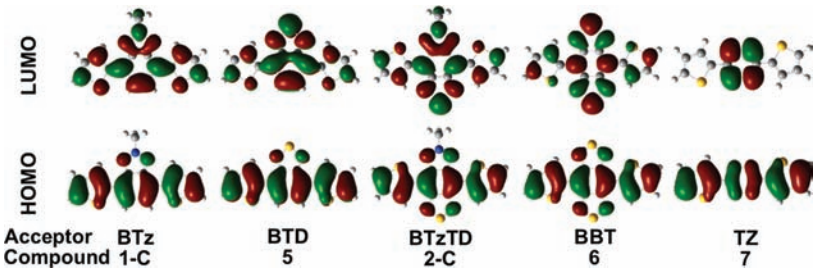

Figure 7. Graphical representation of the computed molecular orbitals for oligomers **1-C**, **2-C**, and **5**–**7**, which are ordered according to the acceptor core.

Computational Analysis: Part 2. To understand how replacement of NCH_3 with S in comparing **BTz** and **BTD** in the core heterocycle ring system increases electron-accepting ability, we chose to visualize the HOMO and LUMO of our oligomer series, shown collectively in Figure 7. When comparing **BTz** oligomer **1-C** and **BTD** oligomer **5**, both molecules show delocalization of the HOMO across the molecule, with the LUMO being shifted more toward the acceptor core. The LUMO for both oligomers assumes a more quinoidal form as shown by the presence of orbital lobes in the bonds between the donor and acceptors. This orbital lobe pattern is similar to the HOMO of a series of thiophene oligomers that are quinoidal in the ground state.[34] As indicated by the bond length and Wiberg bond indices of the C–C bond between the acceptor and thiophene (Table 2), it is considered that **BTz** oligomer **1-C** and **BTD** oligomer **5** have the same degree of quinoidal character, and, thus, this is not the reason for the difference in the LUMO level of these oligomers. Because the LUMOs consist mainly of the π^* orbital on the acceptors, we focused on the computed geometrical difference between **1-C** and **5**. The largest difference between these two molecules is observed in the bond length between the imine nitrogen and the central atoms: the N–N bond length in **1-C** is 1.319 Å, and the N–S bond length in **5** is computed to be 1.630 Å. Other geometrical parameters are summarized in the Supporting Information. It is reasonable to consider that the longer N–S bond decreases the π^* orbital energy. In fact, we find that when we take the optimized geometry of oligomer **5** and replace the central S atom of the **BTD** moeity with NCH_3, while holding all geometrical parameters constant, the LUMO energy is computed to be −2.84 eV in vacuo, which is closer to the computed LUMO energy of **5** (−2.89 eV) than to the computed LUMO value of **1-C** (−2.23 eV). Therefore, we can conclude that, at least partially, the difference in accepting ability between **BTz** and **BTD** stems from the difference in the imine–central atom bond length.

Table 2. Donor–Acceptor C–C[a] Bond Lengths and Wiberg Bond Indices

compound	acceptor	bond length (Å)	Wiberg bond index
1-C	**BTz**	1.454	1.121
5	**BTD**	1.455	1.124
2-C	**BTzTD**	1.445	1.156
6	**BBT**	1.445	1.167

[a]The C–C bond is defined as the bond between the 2-position on thiophene and the acceptor.

Another major difference between the **1-C** and **5** pair of oligomers is the size of the molecular orbital lobe on the central atom in the LUMO. Specifically, the lobe on the central nitrogen atom in **BTz** is much smaller than the lobe on sulfur in **BTD**. We would expect the imine nitrogens to act as electron-accepting atoms, and sulfur, being larger and more polarizable, likely helps to stabilize any charge buildup on these imine nitrogens that arises in the charge transfer state produced by photoexcitation. The central nitrogen in the case of **BTz** is unable to provide as much stabilization as it is smaller and less polarizable, therefore limiting the electron-accepting ability of **BTz**.

The molecular orbitals of **BTzTD** and **BBT** oligomers **2-C** and **6** show features similar to those of the **BTz** and **BTD** oligomers **1-C** and **5**. The HOMO levels are deocalized across the whole of the molecules with the LUMO being localized mostly on the acceptor (Figure 7). Quinoidal character is observed in the LUMO molecular orbitals. However, because the **BTzTD** unit in oligomer **2-C** also has a sulfur atom like the **BTD** and **BBT** units present in **5** and **6**, it has enhanced electron-accepting ability as compared to the **BTz** unit in **1-C**. It should also be noted that the bond lengths and Wiberg bond indices between the acceptor and the donor thiophene are slightly shorter and larger, respectively, in **2-C** and **6** than in **1-C** and **5** as shown in Table 2. Therefore, it is considered that **BTzTD** and **BBT** enhance the quinoidal character as compared to **BTz** and **BTD**.

As a final component to our computational analysis, we compare key bond lengths and Wiberg bond indices, a measure of bond order, for **1-C** and **5** to understand the differences in the electron-accepting ability in this pair (Table 3). A full table of computed bond lengths and bond indices is available in the Supporting Information; we focus here on the C–N and annulated C–C bonds. The annulated C–C bond, which we define as the bond shared by the five- and six-membered rings in the acceptors, in **BTz** oligomer **1-C** is computed to be

Table 3. Selected Bond Lengths and Wiberg Bond Indices for D–A–D Oligomers

		bond length (Å)		Wiberg bond index	
compound	acceptor	annulated C–C	C–N	annulated C–C	C–N
1-C	**BTz**	1.425	1.349	1.223	1.359
5	**BTD**	1.456	1.336	1.152	1.452

dx.doi.org/10.1021/ja207978v | J. Am. Chem.Soc. 2012, 134, 2599–2612

shorter by 0.031 Å than the corresponding bond in **BTD** oligomer **5**. This correlates with a larger annulated C−C bond index in **1-C**, indicating that this bond has greater double bond character in **1-C** when compared to **5**. Correspondingly, the C−N bond lengths are shorter by 0.013 Å in **5** as compared to **1-C**. The bond index for the C−N bonds in **5** is also greater, indicating that they have more double bond character. While specific figures are reported in the Supporting Information, the trend observed for **BTz** and **BTD** extends to the **BTzTD** and **BBT** oligomers examined computationally.

Using bond length and bond index data, we can assemble a resonance picture for oligomers **1-C** and **5**, shown in Figure 8.

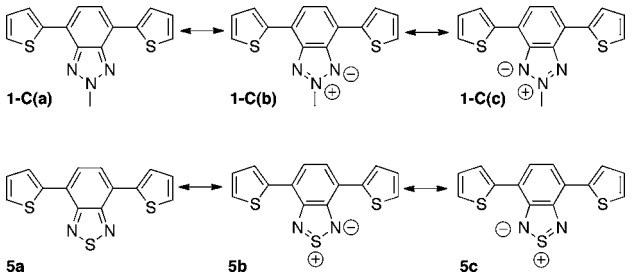

Figure 8. Selected resonance contributors for oligomers **1-C** (top) and **5** (bottom).

The bond lengths and indices suggest that there is some intramolecular charge separation present in both **1-C** and **5**, although the charge separation is greater in **5**. Structures **1-C(b)** and **1-C(c)** allow visualization of this charge separation in the **BTz** oligomer, while **5b** and **5c** demonstrate this charge separation in the **BTD** oligomer. Resonance forms **1-C(b)** and **1-C(c)** seem favorable when considering that the acceptor exists as the annulation of two Clar sextets in the form of a benzene ring and a zwitterionic triazole ring. While the same is true for **5b** and **5c**, the bond length and bond index data suggest that these two resonance forms contribute less than they do in oligomer **1-C**. Because of the enhanced aromatic character in the **BTz** core, breaking that aromaticity requires greater energy. In addition, the conjugation pathway that would allow the two thiophenes to interact via conjugation is partly disrupted by the presence of the aromatic benzene ring. This effect is similar to that seen in a family of oligomers that contain either naphthyl or methano[10]annulene cores.[35] The naphthyl oligomers show shorter wavelength absorption due to the localization of electrons in a benzene structure according to Clar's rule, while the methano[10]annulene oligomers were afforded full delocalization and longer wavelength absorption. Consequently, we believe that because a symmetrically *N*-alkylated **BTz** acceptor will tend toward resonance forms **1-C(b)** and **1-C(c)**, higher energies will be required to break aromaticity. Thus, electron-accepting ability will be lower than in the **BTD** analogues, which have smaller contributions from resonance forms **5b** and **5c**.

Also worthy of mention is the fact that the calculated HOMO levels show a surprising amount of variation (Figure 2) given that the HOMO energy should be dominated by contributions from the thiophene donor units (shown in Figure 1). In fact, to our knowledge, there has been only a small discussion[25] regarding the electron-donating ability moieties generally viewed as electron acceptors, but it appears that across the analogous series we examine, a non-negligible amount of donor character arises from the central N or S heteroatom. **TZ** containing oligomer **7** has the lowest HOMO level among the series regardless of whether the value in vacuo or in dichloromethane is considered. As an explanation, we believe that the HOMO energy is lowered because **TZ** contains only sp^2 hybridized, electron-deficient imine nitrogens and because it lacks any atoms capable of electron donation through lone pairs as in the case N or S in **BTz**, **BTD**, **BTzTD**, and **BBT**. When comparing the closely related **BTD** and **BTz** oligomers, the computations show that **BTz** has the higher HOMO level. This suggests that the nitrogen atom has a larger electron-donating effect when compared to sulfur. A trend can be established when extending this comparison to **BTzTD** and **BBT**, which, similar to **BTz** and **BTD**, differ only by one atom. **BTzTD** has the higher HOMO level when compared to **BBT** in vacuo and in dichloromethane, although the difference is much smaller in dichloromethane. Again, this strongly suggests that nitrogen has a stronger electron-donating effect that raises the HOMO level of **BTzTD** when compared to sulfur in **BBT**. This is not unexpected, however, because the lone pair on the second period nitrogen is likely to have better orbital overlap with the acceptor π-electron system than the lone pair on the larger third period sulfur atom.

X-ray Crystallographic Analysis. With computational and experimental data showing that **BTzTD** has increased electron-accepting ability relative to **BTz**, we turned our attention to characterizing the structures of **2-H**, **2**, **2-E**, and **4**. To identify the structural features that allow **BTzTD** to function as a strong acceptor and to allow comparison with computationally predicted structural features, single crystals of **2** were grown by slow evaporation of an acetone/hexanes solution and then examined by X-ray diffraction techniques. The crystals obtained were small, dark blue needles with oligomer **2** crystallizing in the monoclinic *C*2/*c* space group with eight molecules in the unit cell. The molecular structure and packing are shown in Figure 9 with selected atoms labeled. A full table with bond lengths and angles is supplied in the Supporting Information. It should be noted that, similar to other D−A−D oligomers,[17,36] **2** shows some disorder with respect to the orientation of the thiophene rings relative to the core of the molecule. The molecules pack in extended slip stacks with no obvious edge to face interactions and intermolecular $\pi-\pi$ distances of 3.359 Å, similar to that observed for **BBT** oligomer **6**, which has intermolecular $\pi-\pi$ distances of 3.42 Å.[17] To our knowledge, there have been no crystal structures of D−A−D **BTz** oligomers reported. In our own lab, we have had difficulty obtaining single crystals of **1** and are thus unable to make a direct structural comparison between **BTz** and **BTzTD** containing oligomers at present.

The structure of oligomer **2** is highly planar with a rms deviation from plane of 0.002 Å for the **BTzTD** acceptor core and 0.173 Å for the thiophene−**BTzTD**−thiophene triad. The larger deviation from plane in the triad reflects that the thiophene rings are twisted slightly out of plane. The dihedral angles defined by C12′−C11−C6−-C5 and C8−C7−C3−C4 are small at −0.29° and 5.30°, respectively, showing that there is effective π-overlap between the thiophene donors and the **BTzTD** core. This molecular planarity is driven partly by nonbonded N···S interactions between the thiophene sulfur atoms and the imino nitrogen atoms in the acceptor, a feature that is well-known for other thiophene−acceptor−thiophene and similar triads.[17,37] We observe N···S distances of 2.804−2.963 Å, close to values observed for similar systems.[17,37] In oligomers where such interactions are not possible, the

dx.doi.org/10.1021/ja207978v | *J. Am. Chem.Soc.* 2012, 134, 2599−2612

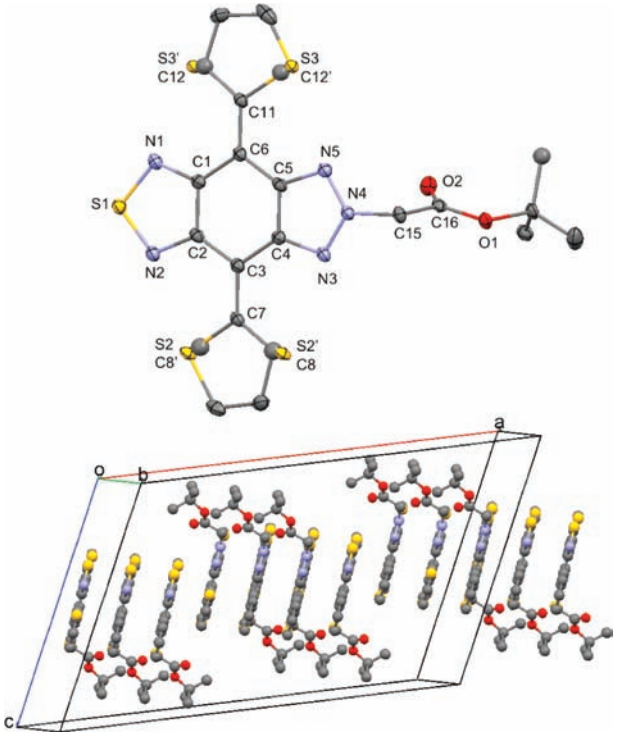

Figure 9. X-ray crystal structure of oligomer **2** (top) and packing diagram showing intermolecular π-stacking (bottom). Thermal ellipsoids are shown at 50% probability. Hydrogen atoms have been omitted for clarity; some molecules have been removed for clarity in the packing diagram. S3', C12', S2', and C8' are the minor parts of the disordered thiophene groups. The rest of the thiophene group atoms are not disordered.

molecules are shown to adopt a structure that is much less planar.[38] The bond lengths of C11−C6 and C7−C3 are 1.453(2) and 1.4564(19) Å, respectively, surprisingly shorter than the value of 1.471(6) Å for the analogous bonds in a related **BBT** oligomer,[17] which indicates that there is a strong donor−acceptor interaction between **BTzTD** and thiophene in the present case. The C−O bond lengths in the ester group (C16−O2 = 1.2043(17) Å and C16−O1 = 1.3306(17) Å) are similar to values expected for an aliphatic ester system,[39] showing this group is electronically isolated from the oligomer π-system due to the presence of the conjugation breaking methylene group.

The bond lengths in the central six-membered ring do not show the bond length pattern (short−long−short−long−long−long) that is expected to result from the benzannulation of the thiadiazole and triazole rings. The two longest bonds in the **BTzTD** six-membered ring are C1−C2 at 1.4579(19) Å and C4−C5 1.4357(19) Å with C1−C2 being longer, which fits with the bond length trend predicted by DFT computations in the **BTz** and **BTD** oligomers. This suggests that there is some local aromatic character in the triazole ring leading to a shortening of C4−C5 relative to C1−C2.

The electron-accepting ability of **BTzTD** can be partly explained by examining the nature of the −N−S−N− framework, as the triazole ring is not expected to play an important role. In the literature, compounds containing **BBT** are usually explicitly described as containing hypervalent sulfur atoms[17,40] or shown containing a −N═S═N− linkage that implies a hypervalent sulfur. Recent reports on polymers containing −N−S−N− linkages along the main chain also imply the need for hypervalent sulfur in the presented molecular schemes.[41] Thus, it is the hypervalent sulfur that is thought to help impart strong electron-accepting ability by allowing the π-electron system to easily adopt a quinoidal structure through D−A interactions.[42] However, as discussed by Leusser and co-workers,[43] it is incorrect to invoke expanded octets in describing sulfur diimide type compounds, and, moreover, the energetics of the sulfur d-orbitals prohibit their participation in bonding, thus precluding an expanded octet. In the case of oligomer **2**, the N(1)−S(1) and N(2)−S(1) bond lengths are longer than would be expected for a N═S double bond,[39,43] indicating significant single bond character. Therefore, we believe that the −N−S−N− linkage is best described as a three-center-four-electron bond. For such a situation, the sulfur atom is expected to bear a formal positive charge, thus making it electron deficient and imparting electron-accepting character on **BTzTD**. This electron deficiency in the ground state would likely drive strong D−A interactions.

Given the bond lengths observed and without invoking hypervalent sulfur, we propose several resonance contributors to the overall observed structure for **2**. These resonance forms are depicted in Figure 10. Structures **A** and **B** depict the three-

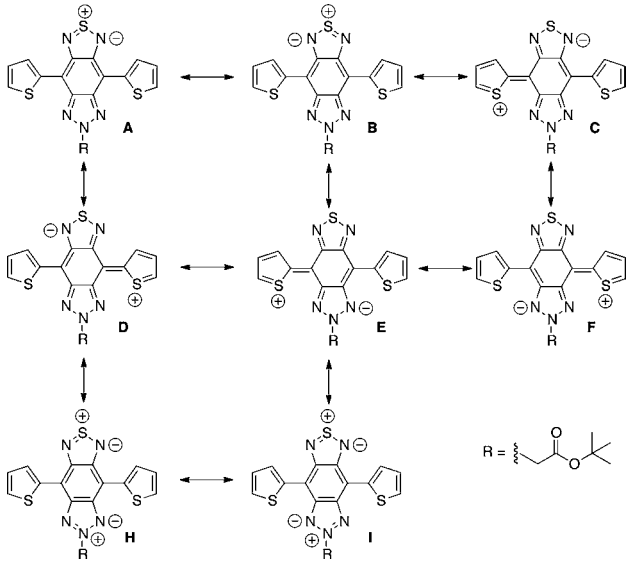

Figure 10. Selected resonance contributors for oligomer **2**.

center-four-electron bond at the −N−S−N− linkage. In both structures, sulfur is electron deficient and bears a formal positive charge, while the more electronegative nitrogen bears a formal negative charge. Structures **C**, **D**, **E**, and **F** account for electron donation from thiophene into either the thiadiazole (**C** and **D**) or triazole (**E** and **F**) rings. In these structures, the thiophene sulfur atoms bear a positive charge, and the imine nitrogens bear a negative charge. Resonance forms **H** and **I** take into account donation of the triazole central nitrogen to the triazole imine nitrogens. In **H** and **I**, a benzene structure is realized in the central six-membered ring as well as an aromatic and zwitterionic triazole ring similar to what was proposed for **BTz** oligomer **1-C** in Figure 8.

To support the resonance forms above, we used natural population analysis (NPA),[44] similar to the work by Leusser,[43] to examine the charge distribution on individual atoms in oligomer **2-C**. The NPA data were obtained as part of our DFT calculations. In particular, we note that sulfur has a computed

dx.doi.org/10.1021/ja207978v | J. Am. Chem.Soc. 2012, 134, 2599−2612

Table 4. Compilation of Photophysical Data for Compounds 1−4

parameter	solvent	1	3	2-H	2	4
λ_{max} (nm)	CH_2Cl_2	278, 387	320, 450	330, 540	336, 630	338, 409, 729
λ_{em} (nm)	CH_2Cl_2	456	516, 546	659	723	870
Φ_F	CH_2Cl_2	0.44[a]	0.32[a]	0.87[b]	0.57[b]	0.06[c]
τ_F (ns)	CH_2Cl_2	2.08 (94%)	1.01	0.73 (12%)	0.44 (4%)	1.16 (73.7%)
		4.12 (6%)		11.1 (88%)	10.3 (96%)	5.06 (26.3%)
Φ_Δ	$CDCl_3$	0.53[d]	0.67[d]	–[e]	–[e]	–[e]
TT_{Abs} (λ/nm)	THF	476	640	–[f]	–[f]	–[f]
TT_{Abs} (ΔA, t = 0)	THF	0.18	0.40	–[f]	–[f]	–[e]
$\tau_{triplet}$ (μs)	THF	46.0	31.1	–[f]	–[f]	–[e]

[a]Measured using coumarin 480 in ethanol (Φ_F = 0.76) as the actinometer.[28] [b]Measured using 3,3′-diethyloxadicarbocyanine iodide in ethanol (Φ_F = 0.49) as the actinometer.[49] [c]Measured using ZnTPP (Φ_F = 0.04 in toluene) as the actinometer.[29] [d]Measured using benzophenone in oxygen-saturated $CDCl_3$ (Φ_Δ = 0.55) as actinometer.[50] [e]Not measured. [f]Transient absorption not observed.

formal charge of +0.912 in vacuo (+0.939 in dichloromethane), while the thiadiazole nitrogens have computed formal charges of −0.627 in vacuo (−0.636 in dichloromethane). Because sulfur is computed to have a formal charge of near unity, it is electron deficient. In the excited state, electron density is transferred from the donor groups to the thiadiazole moiety to alleviate sulfur's electron deficiency; thus, the electron-deficient sulfur is a significant feature that imparts strong electron-accepting ability on **BTzTD**. In contrast, the N−CH_3 nitrogen has a computed formal charge of 0.066 (0.076 in dichloromethane), while the imine nitrogens have computed formal charges of −0.272 (−0.277 in dichloromethane) in **BTz** oligomer. The N−CH_3 unit has a formal charge of 0.344 (0.371 in dichloromethane). In contrast, BTz oligomer **2-C** has smaller formal charges, suggesting that excited-state charge transfer will not occur as easily. A complete list of atom charges is available in the Supporting Information.

Photophysics of Oligomers. To further characterize the optical properties of the oligomers, we explored the solution-phase excited-state dynamics for the **BTz** and **BTzTD** oligomers. All of the oligomers, as discussed previously, show strong fluorescence with moderate to high quantum yields. Fluorescence lifetime measurements reveal that **BTz** containing compounds **1** and **3** have lifetimes (τ_f) in the range of 1−2 ns (Table 4). The radiative decay rates for **1** and **3** calculated by the expression $k_r = \Phi_F/\tau_f$ are in the range (2−3) × 10^8 s^{-1}. The lifetimes and radiative decay rates for the **1** and **3** are typical for π-conjugated oligomers with strongly allowed long-axis polarized π,π^* singlet excited states.[45] By contrast, the **BTzTD** compounds **2-H** and **2** have fluorescence lifetimes that are 1 order of magnitude larger than the **BTz** series compounds ($\tau \approx 10$ ns), and the corresponding radiative rates are significantly less (8 and 6 × 10^7 s^{-1} for **2-H** and **2**, respectively). The significant difference in fluorescence lifetime and radiative rates for **2-H** and **2** likely reflects the fact that the singlet state in the **BTzTD** oligomers has a significant degree of charge transfer character, and it adds support to the notion that the **BTzTD** unit is a strong acceptor. Also notable is the fact that the fluorescence quantum yield for **4** is markedly less than for the other oligomers. This effect is likely due to the energy gap law, where the nonradiative decay rate is increased due to the relatively low energy of the singlet excited state in this oligomer.[46]

Thiophene containing oligomers typically exhibit long-lived triplet excited states that are produced in moderate yield following intersystem crossing from the singlet state that is produced by excitation.[47] To characterize the triplet state for the series of **BTz** and **BTzTD** oligomers that are the focus of the present investigation, nanosecond−microsecond transient absorption spectroscopy was carried out for samples in degassed THF solution at room temperature. As shown in Figure 11, **BTz** containing trimer **1** and pentamer **3** exhibit

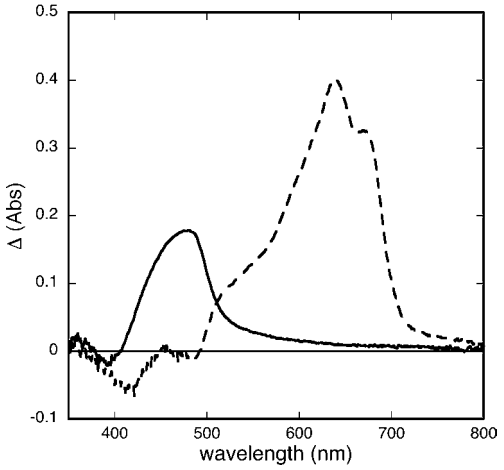

Figure 11. Transient absorption spectroscopy of compounds **1** (−) and **3** (− − −) in THF at room temperature. Spectra obtained at 100 ns delay following a 355 nm, 8 mJ excitation pulse.

strong transient absorption in the mid-visible region following 355 nm excitation. The transient absorption is quenched rapidly by oxygen when the experiment is carried out in air-saturated solution, leading us to assign it to the triplet−triplet absorption of the lowest triplet state. For both oligomers, the triplet state absorption decays with first-order kinetics, and in argon outgassed solution the triplet lifetime is in the 30−50 μs range (Table 4). Although absolute triplet yields were not determined, the significant intensity of the triplet−triplet absorption leads us to conclude that the triplet yield from intersystem from the singlet to the lowest triplet is greater than 0.1, likely due to the significant spin−orbit coupling induced by the thienyl sulfur.[47b] Note that increasing the number of thiophene rings in the oligomer system leads to significant changes in the transient $T_1 \rightarrow T_n$ absorption spectra. Specifically, as compared to trimer **1**, the triplet−triplet absorption of pentamer **3** is red-shifted from 476 to 640 nm and is more intense. The red-shift in the triplet−triplet absorption suggests that the triplet state is more delocalized in the longer oligomer system, and the increase in the absorption implies that the triplet yield is larger in **3**. Note

dx.doi.org/10.1021/ja207978v | J. Am. Chem.Soc. 2012, 134, 2599−2612

that the possibility that the triplet yield is larger in **3** as compared to **1** is consistent with the observation that the fluorescence quantum efficiency is smaller for the longer oligomer (note that fluorescence and intersystem crossing are competing processes, so an increase in one pathway would be reflected by a reduction in the other).

Interestingly, in contrast to the to the **BTz** oligomers, transient absorption spectroscopy of the **BTzTD** containing oligomers **2-H**, **2**, and **4** reveals no observable transient absorption on the nanosecond−microsecond time scale due to a triplet excited state, despite the fact that these two trimers contain thiophene rings as do **1** and **3**. From this observation, we conclude that intersystem crossing in the **BTzTD** oligomers is inefficient, which is surprising given that their fluorescence quantum yields are only slightly higher than those for the **BTz** oligomers. We suspect that the very low intersystem crossing yield in the **BTzTD** oligomers is a consequence of the fact that the singlet excited state has a significant degree of charge-transfer character. Although a previous study explored triplet energies in donor−acceptor oligomers,[48] we are not aware of any previous studies that have correlated the intersystem crossing yield with the degree of donor−acceptor interaction in π-conjugated oligomers or polymers. The interesting observation here that the triplet yield is low for the **BTzTD** oligomers suggests that a systematic study of triplet yields in donor−acceptor oligomers is warranted.

Finally, to further probe the triplet state characteristics of **BTz**, we examined their ability to sensitize singlet oxygen in solution, which should be facile given the strong transient absorption of both **1** and **3** with $\tau_{triplet} > 10$ s. Singlet oxygen ($^1O_2(^1\Delta_g)$) is produced via energy transfer from excited triplet states to molecular oxygen according to the reaction, $^3S^* + O_2(^3\sum_g^-) \rightarrow S + {}^1O_2(^1\Delta_g)$, where S is the (oligomer) sensitizer. The $^1O_2$ that is produced by sensitization is detected by monitoring its emission in the near-infrared region at 1270 nm;[50] moreover, by measuring the singlet oxygen quantum yield (Φ_Δ), it is possible to establish a lower limit for the intersystem crossing yield in the sensitizer.[51] As anticipated, **BTz** oligomers **1** and **3** efficiently sensitize $^1O_2(^1\Delta_g)$, as evidenced by the observation of strong emission at 1270 nm from air-saturated $CDCl_3$ solutions of the oligomers. The quantum yield of sensitized singlet oxygen formation (Φ_Δ) was determined for the two oligomers, and the values for **1** (Φ_Δ = 0.53) and **3** (Φ_Δ = 0.67) are comparatively large. Note that in many cases the singlet oxygen yield is a direct measure of the intersystem crossing efficiency of the sensitizer.[51] Thus, these comparatively large values underscore the fact that intersystem crossing is rather efficient in the **BTz** oligomers. Furthermore, it is interesting to note that for both oligomers the sum of the singlet oxygen yield and the fluorescence yield is close to unity (i.e., $\Phi_F + \Phi_\Delta \approx 1$, Table 4). This fact indicates that for these oligomers the predominant decay pathways for the singlet state are fluorescence and intersystem crossing to the triplet excited state.

SUMMARY AND CONCLUSION

We have shown that the **BTz** moiety, considered an electron acceptor in polymeric systems, does not function as a good electron acceptor in oligomeric systems, which we believe is a consequence of the larger aromatic character of **BTz** relative to other electron acceptors. **BTz** containing molecules show reversible oxidation when examined by cyclic voltammetry, but do not show reductive processes within the useful window of the solvent/electrolyte system employed and show UV and high energy visible transitions that are not indicative of D−A interactions. In contrast, a new acceptor, **BTzTD**, which is a hybrid of **BTz** and **BTD**, proves to be both an excellent electron acceptor as well as a good electron-donating group. While **BTz** containing oligomers absorb mostly in the UV region, the analogous **BTzTD** containing oligomers feature absorption bands that extend into the long wavelength region of the visible spectrum. The **BTzTD** oligomer **2** examined electrochemically shows reduction at a potential slightly negative to that of the conduction band of nanocrystalline TiO_2. The X-ray crystal structure of a **BTzTD** trimer shows a high level of planarity with short D−A bond lengths, suggesting strong coupling across the D−A−D framework. The bond lengths support the idea that the triazole moiety has greater local aromatic character than the thiadiazole moiety. Transient absorption and singlet oxygen emission spectroscopy were used to probe the triplet states of the oligomers. These studies reveal that **BTz** containing oligomers examined show strong triplet−triplet absorption and the triplets can efficiently sensitize the formation of singlet oxygen, implying that the triplet yields are large for both oligomers studied. By contrast, these studies show that the **BTzTD** containing oligomers do not undergo efficient intersystem crossing to produce a triplet excited state.

In conclusion, we have demonstrated the ability to construct donor−acceptor conjugated oligomers, which feature the hybrid **BTzTD** unit in the core. These oligomers exhibit strong visible light absorption as a consequence of the donor−acceptor electronic structure. In preliminary work, we have shown that the acid forms produced by hydrolysis of the *tert*-butyl esters in **1** and **2** readily adsorb to nanocrystalline TiO_2 films. Work in progress seeks to characterize these systems as visible light sensitizers for dye-sensitized solar cell application.

EXPERIMENTAL SECTION

Complete synthetic procedures and NMR characterization for all new compounds as well as specifics on the instrumentation and methods employed are detailed in the Supporting Information.

ASSOCIATED CONTENT

Supporting Information

X-ray crystallographic data for oligomer **2**. Synthetic procedures and NMR characterization for **1**−**4**, **1-E**, **2-E**, **2-H**, **12a**, **13**, **19**, and **20**. Complete list of authors for references. Computational parameters (table of energy values, atomic coordinates, NPA analysis) for oligomers **1-C**, **2-C**, and **5**−**7**. This material is available free of charge via the Internet at http://pubs.acs.org.

AUTHOR INFORMATION

Corresponding Author

kschanze@chem.ufl.edu; reynolds@chemistry.gatech.edu

Present Addresses

[†]Department of Chemistry, University of Illinois at Urbana−Champaign, 600 South Mathews Avenue, Urbana, Illinois 61801, United States.

[#]School of Chemistry and Biochemistry, Georgia Institute of Technology, Atlanta, GA 30332, United States.

ACKNOWLEDGMENTS

Dr. Khalil A. Abboud wishes to acknowledge the National Science Foundation and the University of Florida for funding of the purchase of the X-ray equipment. D.G.P. would like to

thank David Liu for help with aquiring DPV data. D.G.P., F.F., J.R.R., and K.S.S. gratefully acknowledge financial support from the Department of Energy (Grant Number DE-FG-02-96ER14617) for the synthesis and experimental characterization effort. S.H. would like to acknowledge the Camille and Henry Dreyfus Foundation, and Y.-y.O. gratefully acknowledges the National Science Foundation (NSF OCI 1102418) for funding the computational effort.

■ REFERENCES

(1) (a) Nazeeruddin, M. K.; Kay, A.; Rodicio, I.; Humphry-Baker, R.; Müller, E.; Liska, P.; Vlachopoulos, N.; Grätzel, M. *J. Am. Chem. Soc.* **1993**, *115*, 6382−6390. (b) Nazeeruddin, M. K.; Klein, C.; Liska, P.; Grätzel, M. *Coord. Chem. Rev.* **2005**, *249*, 1460−1467. (c) Nazeeruddin, M. K.; Péchy, P.; Renouard, T.; Zyss, J.; Humphry-Baker, R.; Comte, P.; Liska, P.; Cevey, L.; Costa, E.; Shklover, V.; Spicca, L.; Deacon, G. B.; Bignozzi, C. A.; Grätzel, M. *J. Am. Chem. Soc.* **2001**, *123*, 1613−1624.

(2) (a) Amb, C. M.; Chen, S.; Graham, K. R.; Subbiah, J.; Small, C. E.; So, F.; Reynolds, J. R. *J. Am. Chem. Soc.* **2011**, *133*, 10062−10065. (b) Chen, H. Y.; Hou, J. H.; Zhang, S. Q.; Liang, Y. Y.; Yang, G. W.; Yang, Y.; Yu, L. P.; Wu, Y.; Li, G. *Nat. Photonics* **2009**, *3*, 649−653. (c) Wang, E.; Ma, Z.; Zhang, Z.; Vandewal, K.; Henriksson, P.; Inganäs, O.; Zhang, F.; Andersson, M. R. *J. Am. Chem. Soc.* **2011**, *133*, 14244−14247.

(3) Havinga, E. E.; Tenhoeve, W.; Wynberg, H. *Synth. Met.* **1993**, *55*, 299−306.

(4) Roncali, J. *Macromol. Rapid Commun.* **2007**, *28*, 1761−1775.

(5) Mishra, A.; Fischer, M. K. R.; Bauerle, P. *Angew. Chem., Int. Ed.* **2009**, *48*, 2474−2499.

(6) Patel, D. G.; Bastianon, N. M.; Tongwa, P.; Leger, J. M.; Timofeeva, T. V.; Bartholomew, G. P. *J. Mater. Chem.* **2011**, *21*, 4242−4250.

(7) Kira, A.; Matsubara, Y.; Iijima, H.; Umeyama, T.; Matano, Y.; Ito, S.; Niemi, M.; Tkachenko, N.; Lemmetyinen, H.; Imahori, H. *J. Phys. Chem. C* **2010**, *114*, 11293−11304.

(8) Velusamy, M.; Thomas, K. R. J.; Lin, J. T.; Hsu, Y.-C.; Ho, K.-C. *Org. Lett.* **2005**, *7*, 1899−1902.

(9) (a) Balan, A.; Baran, D.; Gunbas, G.; Durmus, A.; Ozyurt, F.; Toppare, L. *Chem. Commun.* **2009**, *44*, 6768−6770. (b) Balan, A.; Gunbas, G.; Durmus, A.; Toppare, L. *Chem. Mater.* **2008**, *20*, 7510−7513. (c) Baran, D.; Balan, A.; Celebi, S.; Esteban, B. M.; Neugebauer, H.; Sariciftci, N. S.; Toppare, L. *Chem. Mater.* **2010**, *22*, 2978−2987. (d) Fang, Q.; Tanimoto, A.; Yamamoto, T. *Synth. Met.* **2005**, *150*, 73−78. (e) Peng, B.; Najari, A.; Liu, B.; Berrouard, P.; Gendron, D.; He, Y.; Zhou, K.; Leclerc, M.; Zou, Y. *Macromol. Chem. Phys.* **2010**, *211*, 2026−2033. (f) Tanimoto, A.; Yamamoto, T. *Adv. Synth. Catal.* **2004**, *346*, 1818−1823. (g) Tanimoto, A.; Yamamoto, T. *Macromolecules* **2006**, *39*, 3546−3552.

(10) Tam, T. L.; Li, H.; Lam, Y. M.; Mhaisalkar, S. G.; Grimsdale, A. C. *Org. Lett.* **2011**, *13*, 4612−4615.

(11) Cozzolino, A. F.; Gruhn, N. E.; Lichtenberger, D. L.; Vargas-Baca, I. *Inorg. Chem.* **2008**, *47*, 6220−6226.

(12) Akbasoglu, N.; Balan, A.; Baran, D.; Cirpan, A.; Toppare, L. *J. Polym. Sci., Part A: Polym. Chem.* **2010**, *48*, 5603−5610.

(13) Liu, L.; Hong, D.-J.; Lee, M. *Langmuir* **2009**, *25*, 5061−5067.

(14) Liu, B. K.; Wu, Q.; Qian, X. Q.; Lv, D. S.; Lin, X. F. *Synthesis* **2007**, *17*, 2653−2659.

(15) Katritzky, A. R.; Pastor, A.; Voronkov, M.; Tymoshenko, D. *J. Comb. Chem.* **2001**, *3*, 167−170.

(16) Seitz, D. E.; Lee, S. H.; Hanson, R. N.; Bottaro, J. C. *Synth. Commun.* **1983**, *13*, 121−128.

(17) Karikomi, M.; Kitamura, C.; Tanaka, S.; Yamashita, Y. *J. Am. Chem. Soc.* **1995**, *117*, 6791−6792.

(18) Steckler, T. T.; Abboud, K. A.; Craps, M.; Rinzler, A. G.; Reynolds, J. R. *Chem. Commun.* **2007**, *46*, 4904−4906.

(19) Wang, E. R.; Hou, L. T.; Wang, Z. Q.; Hellstrom, S.; Mammo, W.; Zhang, F. L.; Inganas, O.; Andersson, M. R. *Org. Lett.* **2010**, *12*, 4470−4473.

(20) Perzon, E.; Zhang, F. L.; Andersson, M.; Mammo, W.; Inganas, O.; Andersson, M. R. *Adv. Mater.* **2007**, *19*, 3308−3311.

(21) Salhi, F.; Lee, B.; Metz, C.; Bottomley, L. A.; Collard, D. M. *Org. Lett.* **2002**, *4*, 3195−3198.

(22) Cramer, C. J. *Essentials of Computational Chemistry: Theories and Models*, 2nd ed.; Wiley: Chichester, West Sussex, England; Hoboken, NJ, 2004.

(23) Audebert, P.; Sadki, S.; Miomandre, F.; Clavier, G.; Vernieres, M. C.; Saoud, M.; Hapiot, P. *New J. Chem.* **2004**, *28*, 387−392.

(24) Zhang, G.; Musgrave, C. B. *J. Phys. Chem. A* **2007**, *111*, 1554−1561.

(25) Price, S. C.; Stuart, A. C.; Yang, L.; Zhou, H.; You, W. *J. Am. Chem. Soc.* **2011**, *133*, 8057−8057.

(26) Fraind, A. M.; Tovar, J. D. *J. Phys. Chem. B* **2010**, *114*, 3104−3116.

(27) Pham, C. V.; Burkhardt, A.; Shabana, R.; Cunningham, D. D.; Mark, H. B.; Zimmer, H. *Phosphorus, Sulfur Silicon Relat. Elem.* **1989**, *46*, 153−168.

(28) Rurack, K.; Spieles, M. *Anal. Chem.* **2011**, *83*, 1232−1242.

(29) Guldi, D. M.; Luo, C. P.; Prato, M.; Dietel, E.; Hirsch, A. *Chem. Commun.* **2000**, *5*, 373−374.

(30) Jayakannan, M.; Van Hal, P. A.; Janssen, R. A. J. *J. Polym. Sci., Part A: Polym. Chem.* **2002**, *40*, 251−261.

(31) Kono, T.; Kumaki, D.; Nishida, J.; Tokito, S.; Yamashita, Y. *Chem. Commun.* **2010**, *46*, 3265−3267.

(32) Bard, A. J.; Faulkner, L. R. *Electrochemical Methods: Fundamentals and Applications*, 2nd ed.; Wiley: New York, 2001; p xxi, 833 p.

(33) (a) Cardona, C. M.; Li, W.; Kaifer, A. E.; Stockdale, D.; Bazan, G. C. *Adv. Mater.* **2011**, *23*, 2367−2371. (b) Thompson, B. Variable Band Gap Poly(3,4-alkylenedioxythiophene)-Based Polymers for Photovoltaic and Electrochromic Applications. Ph.D. Dissertation, University of Florida, Gainesvlle, FL, 2005.

(34) Casado, J.; Zgierski, M. Z.; Ewbank, P. C.; Burand, M. W.; Janzen, D. E.; Mann, K. R.; Pappenfus, T. M.; Berlin, A.; Perez-Inestrosa, E.; Ortiz, R. P.; Navarrete, J. T. L. *J. Am. Chem. Soc.* **2006**, *128*, 10134−10144.

(35) Peart, P. A.; Tovar, J. D. *Org. Lett.* **2007**, *9*, 3041−3044.

(36) Kitamura, C.; Tanaka, S.; Yamashita, Y. *Chem. Mater.* **1996**, *8*, 570−578.

(37) Akhtaruzzaman, M.; Kamata, N.; Nishida, J.; Ando, S.; Tada, H.; Tomura, M.; Yamashita, Y. *Chem. Commun.* **2005**, *25*, 3183−3185.

(38) Akhtaruzzaman, M.; Tomura, M.; Nishida, J.; Yamashita, Y. *J. Org. Chem.* **2004**, *69*, 2953−2958.

(39) Allen, F. H.; Kennard, O.; Watson, D. G.; Brammer, L.; Orpen, A. G.; Taylor, R. *J. Chem. Soc., Perkin Trans. 2* **1987**, S1−S19.

(40) Ono, K.; Tanaka, S.; Yamashita, Y. *Angew. Chem., Int. Ed. Engl.* **1994**, *33*, 1977−1979.

(41) (a) Wang, M. F.; Sun, Y. M.; Tong, M. H.; Chesnut, E. S.; Seo, J. H.; Kumar, R.; Wudl, F. *J. Polym. Sci., Part A: Polym. Chem.* **2011**, *49*, 441−451. (b) Wang, M. F.; Wudl, F. *J. Mater. Chem.* **2010**, *20*, 5659−5663.

(42) Salzner, U.; Karalti, O.; Durdagi, S. *J. Mol. Model.* **2006**, *12*, 687−701.

(43) Leusser, D.; Henn, J.; Kocher, N.; Engels, B.; Stalke, D. *J. Am. Chem. Soc.* **2004**, *126*, 1781−1793.

(44) Reed, A. E.; Curtiss, L. A.; Weinhold, F. *Chem. Rev.* **1988**, *88*, 899−926.

(45) Walters, K. A.; Ley, K. D.; Cavalaheiro, C. S. P.; Miller, S. E.; Gosztola, D.; Wasielewski, M. R.; Bussandri, A. P.; van Willigen, H.; Schanze, K. S. *J. Am. Chem. Soc.* **2001**, *123*, 8329−8342.

(46) (a) Caspar, J. V.; Meyer, T. J. *J. Phys. Chem.* **1983**, *87*, 952−957. (b) Henry, B. R.; Siebrand, W. In *Organic Molecular Photophysics*; Birks, J. B., Ed.; J. Wiley: New York, 1973.

(47) (a) de Melo, J. S.; Silva, L. M.; Arnaut, L. G.; Becker, R. S. *J. Chem. Phys.* **1999**, *111*, 5427−5433. (b) Zhou, Z.; Corbitt, T. S.;

Parthasarathy, A.; Tang, Y.; Ista, L. F.; Schanze, K. S.; Whitten, D. G. *J. Phys. Chem. Lett.* **2010**, *1*, 3207−3212.
(48) Karsten, B. P.; Bijleveld, J. C.; Viani, L.; Cornil, J.; Gierschner, J.; Janssen, R. A. J. *J. Mater. Chem.* **2009**, *19*, 5343−5350.
(49) Dempster, D. N.; Thompson, G. F.; Morrow, T.; Rankin, R. *J. Chem. Soc., Faraday Trans.* **1972**, *68*, 1479−1496.
(50) Wilkinson, F.; Helman, W. P.; Ross, A. B. *J. Phys. Chem. Ref. Data* **1993**, *22*, 113−262.
(51) Burrows, H. D.; de Melo, J. S.; Serpa, C.; Arnaut, L. G.; Monkman, A. P.; Hamblett, I.; Navaratnam, S. *J. Chem. Phys.* **2001**, *115*, 9601−9606.